AJNR Am J Neuroradiol 23:1466–1474, October 2002

New Syndrome Characterized by Hypomyelination with Atrophy of the Basal Ganglia and Cerebellum

Marjo S. van der Knaap, SakkuBai Naidu, Petra J.W. Pouwels, Simona Bonavita, Rudy van Coster, Lieven Lagae, Jürgen Sperner, Robert Surtees, Raphael Schiffmann, and Jakob Valk

BACKGROUND AND PURPOSE: Leukoencephalopathies of unknown origin constitute a considerable problem in child neurology. The purpose of our ongoing study of the subject was to define new disease entities among them by using primarily MR imaging pattern recognition.

METHODS: **We identified seven unrelated patients with a distinct MR imaging pattern consisting of hypomyelination and atrophy of the basal ganglia (neostriatum) and cerebellum (H-ABC). We reviewed the clinical, MR imaging, MR spectroscopic, and laboratory data.**

RESULTS: **Clinically, the patients' diseases were characterized by variably disturbed early development followed by increasing extrapyramidal movement abnormalities, ataxia, and spasticity. Mental capacity was variably affected, but it appeared to be relatively preserved. Parents were not related, and none of their siblings were affected. No metabolic defect was found. Follow-up MR imaging demonstrated atrophy of the cerebral white matter, neostriatum, and cerebellum, which was most pronounced in the most clinically severe cases. Single-voxel proton MR spectroscopic results were normal in the parietal cortex. In the cerebral white matter, myo-inositol and creatine levels were elevated; this finding was compatible with gliosis. *N*-acetylaspartate and choline levels were normal, suggesting that neither axonal loss nor active demyelination occurred. Proton MR spectroscopic imaging revealed relatively decreased *N*-acetylaspartate levels in the frontal region.**

CONCLUSION: **The uniform and highly characteristic MR imaging findings, in combination with the similarities in the clinical findings, provide evidence of a distinct nosologic entity. The acronym H-ABC is offered to indicate patients sharing these clinical and MR imaging features.**

Leukoencephalopathies of unknown origin constitute a vexing problem in child neurology. Despite ongoing extensive investigations, specific diagnosis is still elusive in at least 50% of children with a leukoencephalopathy (1, 2). In a recent survey of MR imaging findings in childhood leukoencephalopathies of unknown origin, hypomyelinating disorders constituted the largest single category (1). Hypomyelination refers to a substantial deficit in myelin deposition, as compared with normal amount, and it may be caused by either delayed myelination or a permanent lack of myelin. Congenital hypomyelinating neuropathies are disorders characterized by a permanent lack of myelin sheaths in the peripheral nerves (3, 4). By analogy, the term hypomyelinating disorders can be used for leukoencephalopathies characterized by a permanent deficit in myelin deposition in the brain. Permanent hypomyelination and delayed myelination have similar appearances on a single MR imaging study, but sequential studies can distinguish the two, showing evidence of an increasing myelin content in delayed myelination but unchanged myelin deficiency in hypomyelinating disorders.

Several hypomyelinating disorders are known. These include Pelizaeus-Merzbacher disease (5, 6),

Received November 15, 2001; accepted June 6, 2002.

From the Departments of Child Neurology (M.S.v.d.K.), Clinical Physics and Informatics (P.J.W.P.), and Radiology (J.V.), Free University Medical Center, Amsterdam, the Netherlands; the Department of Neurogenetics, Kennedy Krieger Institute, Baltimore, MD (S.N.); the Neuroimaging Branch (S.B.) and the Developmental and Metabolic Neurology Branch (R.S.), the National Institutes of Health, Bethesda, MD; the Department of Pediatric Neurology, Universitair Ziekenhuis C. Hooft, Gent, Belgium (R.v.C.); the Department of Pediatric Neurology, Universitair Ziekenhuis Gasthuisberg, Leuven, Belgium (L.L.); the Department of Pediatrics, Universitäts-klinikum, Lübeck, Germany (J.S.); and Department of Pediatric Neurology, Great Ormond Street Hospital, London, England (R.S.).

Address reprint requests to Marjo S. van der Knaap, Department of Child Neurology, Free University Medical Center, P.O. Box 7057, 1007 MB Amsterdam, the Netherlands.

TABLE 1: Clinical History and Present Findings

Finding	Patient						
	1	2	3	4	5	6	7
Sex	Male	Male	Female	Female	Female	Male	Male
Year of birth	1993	1991	1989	1989	1989	1983	1980
No. siblings							
Affected	0	0	0	0	0	0	0
Unaffected	0	0	1	0	0	2	2
Consanguinity of parents	No	No	No	No	No	No	No
Ethnic background	Caucasian	Caucasian	Caucasian	Caucasian	Asian-Caucasian	Caucasian	Caucasian
Age at presentation	1 y	1.5 y	2 y	1 y	2 mo	2 mo	3 y
Presenting sign	Delayed motor development	Delayed motor development	Delayed motor development	Delayed motor development	Poor vision	Poor vision	Motor deterioration
Initial motor development	Delayed	Delayed	Delayed	Normal	Very little*	Very little*	Normal
Supported walking	At 3.5 y	At 18 mo	At 20 mo	At 12 mo	No	No	At 12 mo
Unsupported walking	No	No	At 2.5 y	No	No	No	At 14 mo
Onset of motor deterioration	At 1.5 y	At 2 y	At 6 y	At 2 y	In infancy	At 5 mo	At 3 y
Loss of supported walking ability	None	At 4.5 y	At 6 y	At 2.5 y	NA	NA	At 10 y
Motor signs							
Spasticity	Yes	Yes	Yes	Yes	Yes	Yes	Yes
Ataxia	Yes, mild	Yes	Yes	Yes	Not testable	Not testable	Yes, mild
Tremor	No	Yes	Yes	No	No	No	Yes
Choreoathetosis	No	Yes	Yes	Yes	Yes	No	Yes
Dystonia	Yes	Yes	Yes	Yes	Yes	No	Yes
Rigidity	Yes	Yes	No	Yes	Yes	Yes	Yes
Dysarthria	Anathria	Yes	Yes	Anarthria	Anarthria	Anathria	Yes
Intelligence	Mental retardation	Learning difficulties	Learning difficulties	Learning difficulties	Not testable	Not testable	Learning difficulties
Cognitive decline	No	Questionable	Questionable	No	Not testable	Not testable	Mild
Epilepsy	No	No	No	No	Few seizures	One seizure	No
Vision	Normal	Normal	Normal	Normal	Decreased, pale optic discs	Decreased, pale optic discs	Normal
Hearing	Normal	Normal	Normal	Normal	Normal	Normal	Normal
Head circumference	−2 SD	Normal	Normal	Normal	<2 SD	<2 SD	Normal
Stature	<2 SD	Normal	Normal	Normal	<2 SD	<2 SD	Normal

Note.—NA indicates not applicable.

* Holding objects.

Salla disease (7), Cockayne syndrome type II (8), and Tay syndrome (9). Patients with a hypomyelinating disorder of unknown origin have a highly variable clinical picture; therefore, these disorders are unlikely to represent a single disease entity (1).

The purpose of our ongoing multi-institutional study on the MR imaging of leukoencephalopathies of unknown origin was to identify and define novel disease entities (1, 10). When a group of patients have a distinct and homogeneous pattern of MR imaging abnormalities, their clinical features and laboratory findings are studied to confirm the homogeneity of the patient group. This approach has been successful in identifying and defining megalencephalic leukoencephalopathy with subcortical cysts (11) and vanishing white matter (12, 13). With both subcortical cysts and vanishing white matter, the responsible gene defects were recently identified (14–16). This discovery confirms the value and validity of this MR imaging–oriented approach.

In the context of this ongoing study, we identified seven patients with a syndrome characterized by hypomyelination and selective atrophy of the neostriatum and cerebellum. We reviewed the clinical, MR imaging, MR spectroscopic, and laboratory findings in these patients to assess the likelihood that they have a distinct nosologic entity.

Methods

To date, our study of unclassified leukoencephalopathies includes 462 patients. Almost all patients who come to our attention live in North America or Western Europe. MR images of patients with a leukoencephalopathy of unknown origin are systematically analyzed and scored (1, 10) and subsequently classified according to the predominant feature or location of the white matter abnormalities (1). Within the category of hypomyelinating disorders, which involves 102 patients, the findings in seven patients were notable because of the absence of a visible putamen, without evidence of a lesion in the region (Table 1). The MR imaging studies and laboratory findings of these patients were collected for further analysis. For all patients, clinical data were recorded (Table 1). Related to the retrospective nature of our study, the clinical and laboratory evaluations of the patients were not uniform. Different expe-

rienced child neurologists (M.S.v.d.K., S.N., R.v.C., L.L., J.S., R.Su., R.Sc.) examined the patients.

In the seven patients, 25 MR imaging examinations were performed on a 1.5-T unit. On each occasion, T1-weighted (T1W) (TR/TE, 570/14) and T2-weighted (T2W) (3000/20, 60, 120) images were obtained in sagittal and transverse planes. They were scored for the stage of myelination, the presence of gray matter and white matter signal intensity abnormalities, and atrophy, according to a previously published protocol (1, 10). In this protocol, a list of 68 items is used, including both anatomic structures and lesional characteristics (1). All items are dichotomized (structures were defined as normal or abnormal; features, present or absent) (1). We subdivided findings involving the decreased volume of a structure into absent, mild (but evident), and severe results. In the case of doubt between absent versus mild or mild versus severe results, the more normal score was used. Two investigators (M.S.v.d.K., J.V.) independently scored the findings, and a consensus was reached when their interpretations differed.

Two patients underwent multiple single-voxel proton (^{1}H) MR spectroscopy on the same 1.5-T MR unit. Volumes-of-interest (VOIs) were selected in the basal ganglia on the left side (4.5 mL), the left parietal white matter (4.5 mL), the midparietal cortex (10 mL), and the cerebellar vermis (6.4 mL). In each VOI, a fully relaxed short-TE stimulated-echo acquisition mode spectrum (TR/TE/mixing time/acquisitions, 6000/20/10/64) was obtained. Metabolite concentrations were calculated by using the LCModel (17, 18) and expressed in units of millimole per liter VOI. Data were compared with values obtained in age-matched control subjects (n = 13; age range, 5–10 years; mean age, 7.1 years) (19).

One patient underwent 1.5-T ^{1}H-MR spectroscopy on two occasions by using the previously described data acquisition (20), and postprocessing procedures (21). A TR/TE of 2200/272 was used (20). We acquired four 15-mm-thick axial sections with a 32 × 32 array of spectra from the voxels, nominate volume of 0.84 mL (7.5 × 7.5 × 15 mm), and 3-mm intersection gap. Metabolite maps were calculated; each represented the distribution of one of the major metabolites. Corresponding conventional MR imaging sections were used to identify anatomic structures (21).

Results

Clinical Profiles

The clinical data are summarized in Table 1. From the beginning, patients 5 and 6 had a more severe clinical picture. They presented with poor vision and absent motor development when they were a few months old. Over the years, signs of spasticity, particularly extrapyramidal movement abnormalities with rigidity, dystonia, and choreoathetosis increased. Both patients seemed to have better mental function than motor function, and they appeared to have social awareness.

In comparison, patients 1–4 and 7 had better early development. Patients 3 and 7 were able to walk unsupported, but their stride was always unstable, and they frequently fell. The remaining three patients were able to walk with support, but patient 1 had great difficulty walking. Motor deterioration set in after several years, with increasing spasticity; ataxia; and, particularly, extrapyramidal movement abnormalities with dystonia, choreoathetosis, and rigidity. All five patients had learning difficulties and required special education, but further cognitive decline was questionable and, at most, minor.

None of the seven patients had other abnormalities at physical examination.

Laboratory Investigations

In all patients, results of routine hematology and chemistry panels were normal. Blood levels of creatine kinase (patients 1–4 and 7), uric acid (patients 1, 4, 6, 7), blood gases (patient 3), ammonia (patients 1–3), vitamin E (patients 3–5), vitamin B_{12} (patients 1, 4, 5), folic acid (patients 4, 5), and copper and ceruloplasmin (patients 2, 4, 6, 7) were normal. Thyroid function (patients 1, 2, 5, 7) was normal. Karyotypes in the blood cells were normal (patients 2, 4–6). Urinary levels of organic acids (patients 1–7), amino acids (patients 1–7), oligosaccharides (patients 2, 3, 5), sialic acid (patients 1, 3, 5, 7), and sulfatides (patients 1, 3) were normal. Serum levels of lactate and pyruvate and plasma levels of amino acids, very-long-chain fatty acids, and phytanic acid were normal in all patients. Transferrin iso-electric focusing showed normal results (patients 1–3). Total and free plasma carnitine levels were normal (patients 1, 3, 4, 7). In all patients, assessment of lysosomal enzymes in white blood cells showed normal levels of arylsulfatase A (metachromatic leukodystrophy), galactocerebrosidase (Krabbe disease), β-galactosidase (GM_1 gangliosidosis), hexosaminidase A (GM_2 gangliosidosis), α-mannosidase (mannosidosis), and fucosidase (fucosidosis). Normal filipin staining in fibroblasts and normal cholesterol esterification ruled out Niemann-Pick type C (patient 7). Analysis of mitochondrial DNA did not reveal mutations or deletions (patients 2, 7). Analysis of mitochondrial function in muscle tissue (patients 1, 7) did not reveal abnormalities. DNA analysis for Pelizaeus-Merzbacher disease was unrevealing (patients 1, 2, 4, 7). CSF analysis revealed normal cell counts and protein levels (patients 1–4, 6, 7) and normal lactate (patients 1–4, 6, 7), amino acid (patients 1, 2, 4, 7), and organic acid (patient 2) levels. CSF levels of monoamines (patient 2), gamma-aminobutyric acid (patients 2, 3), homovanillic acid (patients 2, 3), 5-hydroxyindole-3-acetic acid (patients 2, 3), and 3-methoxytyrosine (patient 3) were normal.

Other Examinations

Ophthalmologic findings were normal in patients 1–4 and 7, but they revealed pale optic disks in patients 5 and 6. Electroretinograms were normal in patients 4–6, whereas visual evoked responses were delayed. Electroencephalography revealed slowing of background activity in all patients. Somatosensory evoked potentials with stimulation of median and tibial nerves were highly delayed in patient 2. In patients 5 and 7, brain stem auditory evoked potentials showed a recordable wave I, whereas all subsequent waves were absent. In patient 2, only waves I and II could be recorded on the right, and waves I–III were recorded on the left. In patients 4 and 6, all waves later than the wave I were recordable but delayed. Motor and sensory nerve conduction veloc-

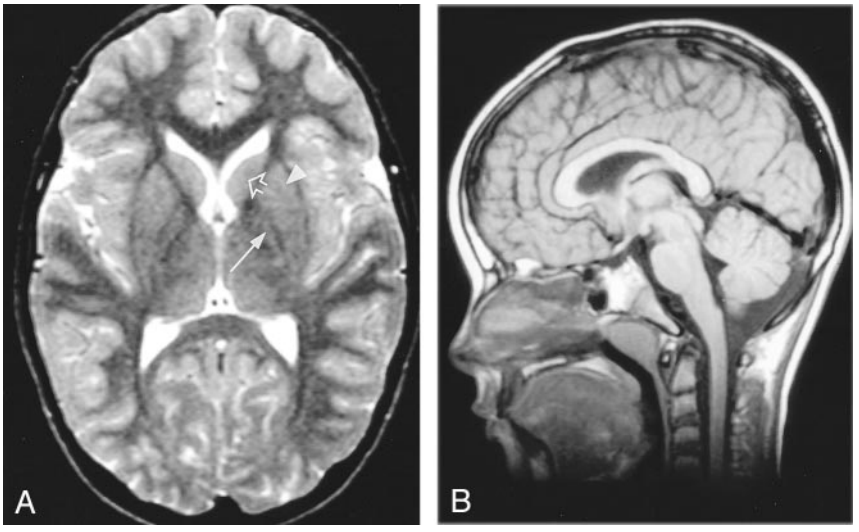

FIG 1. MR images in a healthy 8-year-old boy.

A, Axial T2W image (3000/120). The myelinated white matter has low signal intensity. Note that the normal putamen is a large nucleus (*arrowhead*), whereas the normal globus pallidus is small (*solid arrow*). Also note the normal size of the head of the caudate nucleus (*open arrow*).

B, Sagittal T1W image (570/14). Note the normal size of cerebellar vermis and the corpus callosum.

ities were normal in patients 2, 3, and 5–7. Electromyographic findings were normal in patients 6 and 7.

Sural nerve biopsy revealed no abnormalities in patients 1 and 6. In particular, no abnormalities in the density of myelin sheaths were found at electron microscopy. Light and electron microscopic examination of conjunctival (patients 4, 6) and rectal (patient 6) biopsy samples did not show evidence of storage or abnormal inclusions. Electron microscopy of skin and buffy coat samples did not reveal any abnormalities (patient 7).

MR Imaging

The first MR imaging study was performed at the ages of 1½, 2½, 8, 2½, 1, 3½, and 11 years in patients 1, 2, 3, 4, 5, 6, and 7, respectively. These studies showed a homogeneous picture, with diffuse myelin deficiency as the most striking finding. In all patients, the cerebral white matter, including the corpus callosum and internal capsule, had high signal intensity on T2W images (Figs 1A, 2A, and 3A). Only in patient 1, the corpus callosum and internal capsule had partially low signal intensity (Fig 2A). The cerebellar white matter was either hyperintense or isointense relative to the cortex. The brain stem had low signal intensity, with the exception of the pyramidal tracts in the midbrain and pons, which had high signal intensity (Fig 4). On T1W images, the signal intensity of the cerebral white matter varied from slightly hypointense to slightly hyperintense relative to the cortex. Only in patient 6 was the volume of the cerebral white matter severely decreased, with enlarged lateral ventricles.

In all patients, mild to severe cerebellar atrophy affected the vermis more than the hemispheres. The thalamus and globus pallidus had a normal appearance in all patients. In patient 1, the putamen was abnormally small (Fig 2A). In all other patients, no putamen was visible (Fig 3A). In patients 1–5 and 7, the head of the caudate nucleus had either a normal size (Fig 2A), or it was mildly reduced in size (Fig 3A). In patient 6, the head of the caudate nucleus was entirely flat.

Follow-up MR imaging studies were obtained in patient 1 (three studies at ages 2–6 years), patient 2 (four studies at ages 3½–9 years), patient 3 (one study at 11 years), patient 4 (five studies at ages 3–9 years), patient 5 (two studies at ages 5–11 years), and patient 7 (three studies at ages 15–20 years). The parents of patient 6 refused further MR examination. The follow-up studies revealed that the signal intensity in the white matter remained unchanged, whereas cerebellar atrophy had worsened (Figs 2D and 3D compared with Figs 2B and 3B).

Patients 5 and 7 had the longest follow-up (10 and 9 years, respectively). In patient 5, who had severe clinical signs, the lateral ventricles became markedly enlarged because of a severe loss of white matter; the head of the caudate nucleus disappeared, and the cerebellum became severely atrophic (Figs 3C and D). In patient 7, who had milder clinical signs, the lateral ventricles became slightly enlarged because of mild white matter volume loss. The head of the caudate nucleus became mildly reduced in size. Mild progression of the cerebellar atrophy was observed.

During follow-up in the remaining patients, the putamen became smaller in patient 1, and it was no longer discernible at the age of 4 years (Fig 2C). He had been the only patient with a small but visible putamen on the first MR imaging study. The head of the caudate nucleus decreased in size (Fig 2C). In patient 4, the lateral ventricles became slightly enlarged. In patients 2 and 4, the head of the caudate nucleus decreased in size.

MR Spectroscopy

Single-voxel MR spectroscopic results in patients 2 and 3, obtained when they were aged 7 and 10 years, respectively, are presented in Table 2 and Fig 5. The spectra from the parietal cortex were normal. In the parietal white matter, total *N*-acetylaspartate (NAA) and choline (Cho) levels were normal, whereas myo-

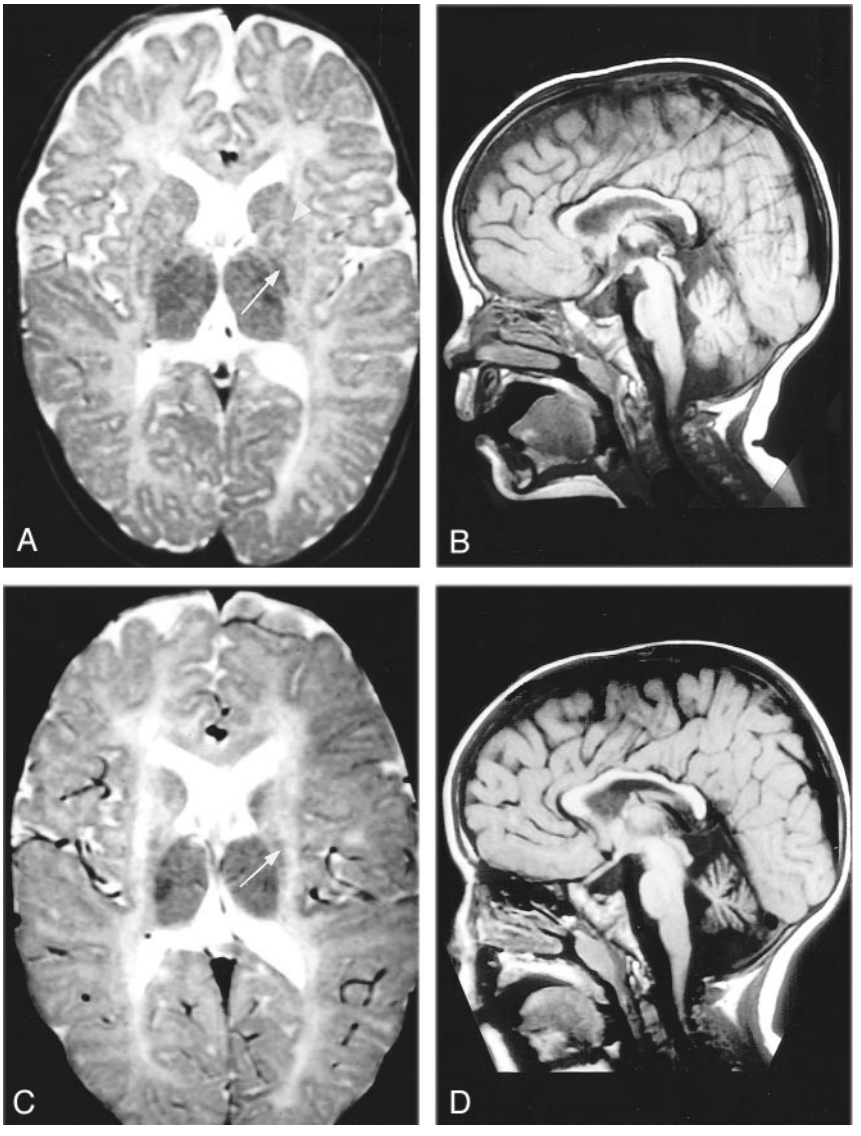

FIG 2. MR images in patient 1, who had disease with intermediate clinical severity.

A, Axial T2W image (3000/120), patient aged 18 months. The cerebral white matter contains little myelin. The putamen is mildly reduced in size (*arrowhead*). The thalamus, caudate nucleus, and globus pallidus (*arrow*) have a normal size.

B, Sagittal T1W image (570/14), patient aged 18 months. The cerebellar vermis is slightly atrophic.

C, Axial T2W image (3000/20, 60, 120), patient aged 6 years. At 6 years, the hypomyelination of the cerebral white matter is unchanged. The putamen is no longer visible. The head of the caudate nucleus is mildly reduced in size. The thalamus and globus pallidus (*arrow*) are normal.

D, Sagittal T1W image (570/14), patient aged 6 years. The cerebellar atrophy has increased.

inositol and total creatine (Cr) were elevated (Fig 5). The spectra obtained from the basal ganglia showed a normal or mildly decreased level of NAA, whereas the myo-inositol level was elevated. The spectra obtained from the cerebellar vermis revealed very low levels of all metabolites. This finding was related to considerable partial volume effects of cerebrospinal fluid associated with the atrophy. To compensate for this effect, the ratio of the metabolite levels to the Cr level was calculated. Relative to the creatine level, the NAA level was decreased and the myo-inositol level was increased in both patients.

In patient 7, ^{1}H MR spectroscopic imaging was performed at the ages of 16 and 20 years. On both occasions, the NAA metabolite map showed that levels in the frontal region were lower than levels in the parieto-occipital region. In all areas, the NAA/Cr values were slightly lower on the second occasion than on the first. The Cho and Cr metabolite maps showed no abnormal regional variation and no change over time.

Discussion

Definition of the H-ABC Syndrome

The MR imaging pattern observed in the present patients consisted of a combination of hypomyelination and atrophy of the basal ganglia and cerebellum (H-ABC). This pattern is distinct from MR imaging patterns observed in other white matter disorders (1, 22) and forms the basis for the definition of this syndrome. White matter that contains no or little myelin has a long T1 and T2, which results in low signal intensity on T1W images and high signal intensity on T2W images (23, 24). With myelin deposition, T1 shortening occurs earlier and is more pronounced, compared with T2 shortening (23, 24). Because of this effect, diffuse deposition of a small amount of myelin results in high signal intensity on T2W and intermediate or high signal intensity on T1W images (1). The MR imaging findings in our patients are compatible with diffuse hypomyelination of the cerebral hemispheres. In addition, the myelin deficit specifically

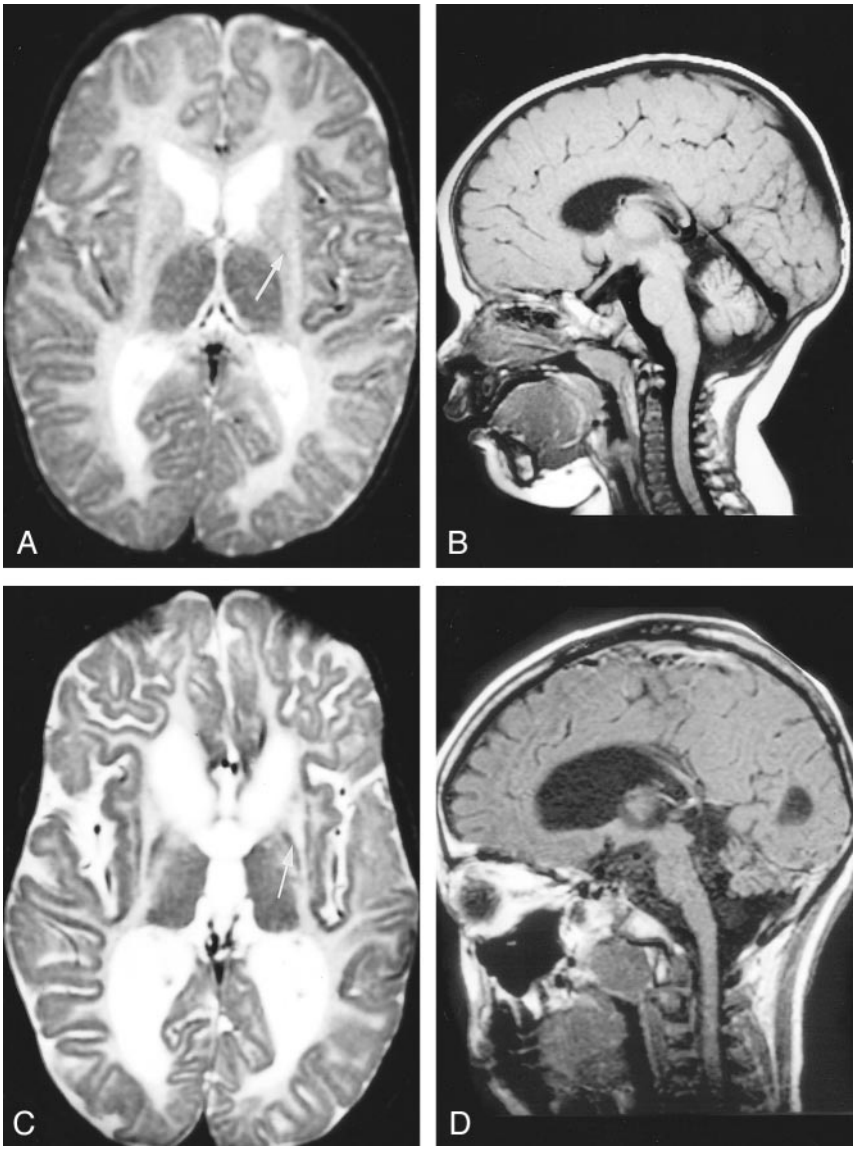

FIG 3. MR images in patient 5, who had severe clinical disease.

A, Axial T2W image (3000/120), patient aged 11 months. At 11 months, little evidence of myelin deposition is present. The thalamus has a normal size. The globus pallidus (*arrow*) is depicted at a slightly higher level than on the other images and is seemingly smaller, but it has a normal size on a lower section (not shown). No visible putamen is present, and the head of the caudate nucleus is small.

B, Sagittal T1W image (570/14), patient aged 11 months. The cerebellar vermis is slightly reduced in size.

C, Axial T2W image (3000/120), patient aged 11 years. At 11 years, the cerebral white matter still contains little myelin. The volume of the white matter has decreased considerably. The head of the caudate nucleus is no longer visible, whereas the globus pallidus (*arrow*) and thalamus appear to be of normal size.

D, Sagittal T1W image (570/14), patient aged 11 years. The cerebellar atrophy has progressed.

involves the pyramidal tracts through the posterior limb of the internal capsule to the brainstem, in which other structures are well myelinated. Considering that no atrophy or further signal intensity change of the pyramidal tracts occur in the brain stem over time, their observed signal intensity abnormalities are unlikely to be secondary to axonal loss. Hypomyelination of the entire pyramidal tracts is unusual. The volume of the cerebral white matter variably decreases over time. Of the basal ganglia, only the neostriatum appears to be affected. In all patients, the putamen was small or absent at the earliest time point. The head of the caudate nucleus initially has a normal or mildly reduced size, and its size decreases further over time until the head of the caudate nucleus becomes entirely flat in severely affected patients. No evidence suggests a reduction in the size of the thalamus or globus pallidus.

Although the severity of the clinical picture varied among the patients, the overall pattern was similar. The severe end of the clinical spectrum is represented in patients 5 and 6. The disease in patient 7 represents a milder variant, whereas those of patients 1–4 represent variants of intermediate severity. In all patients, extrapyramidal movement abnormalities are prominent, ranging from rigidity to choreoathetosis and dystonia. The presence of clinically prominent extrapyramidal signs is highly unusual in patients in whom hypomyelination is the most striking feature on MR images. The clinical picture of such patients is commonly dominated by cerebellar ataxia and spasticity.

The clinical symptoms are correlated with the abnormalities on MR images. The atrophy of the neostriatum is correlated with the extrapyramidal movement abnormalities, the hypomyelination of the pyramidal tracts might be correlated with the spasticity, and the cerebellar atrophy is correlated with cerebellar ataxia. The pale optic disks and decreased vision are probably secondary to hypomyelination. Compared with the mildly affected patients, the severely affected patients develop more pronounced atrophy of the cerebral white matter, cerebellum, and caudate nucleus.

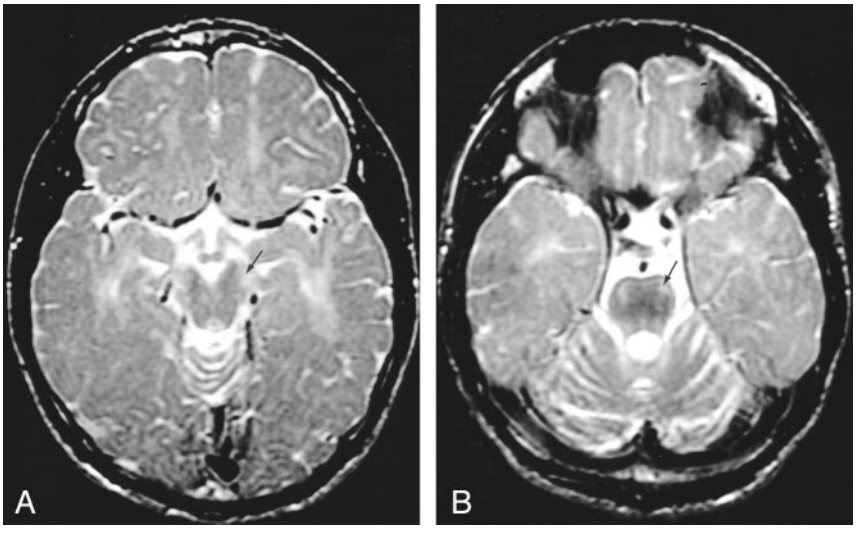

FIG 4. Axial T2W images (3000/120) obtained through the brain stem in patient 7 at the age of 16 years.

A, Note the high signal intensity of the pyramidal tracts in the midbrain (*arrow*).

B, Note the high signal intensity of the pyramidal tracts in the pons (*arrow*).

TABLE 2: MR spectroscopic findings

Level, mmol/L VOI	Patient 2*	Patient 3†	Control Subjects‡
Cerebral cortex			
NAA	8.2	8.2	8.2 (0.9)
Cr	6.0	6.2	6.2 (0.5)
Cho	1.1	1.1	1.2 (0.2)
myo-Ins	4.7	4.5	4.6 (0.7)
Cerebral white matter			
NAA	6.5	7.8	6.9 (0.6)
Cr	5.9	6.4	4.9 (0.4)
Cho	1.3	1.7	1.6 (0.3)
myo-Ins	7.6	8.2	3.7 (0.6)
Basal ganglia			
NAA	6.9	7.6	8.3 (0.8)
Cr	7.0	7.2	7.6 (0.6)
Cho	1.9	1.8	1.9 (0.2)
myo-Ins	6.3	5.9	4.1 (0.74)
Cerebellar vermis§			
NAA	3.50/0.70	2.9/0.71	7.8 (0.8)/0.89 (0.04)
Cr	4.9 /1	4.1/1	8.7 (0.7)/1
Cho	1.3 /0.26	1.5/0.37	2.1 (0.3)/0.25 (0.02)
myo-Ins	5.8 /1.18	4.1/1.00	5.8 (0.3)/0.67 (0.03)

Note.—Cho indicates choline-containing compounds; Cr, creatine; myo-ins, myo-inositol; NAA, N-acetylaspartate.

* Age, 7 y.

† Age, 10 y.

‡ Age range, 5–10 years. Data are the mean (SD).

§ Data are the concentrations relative to Cr.

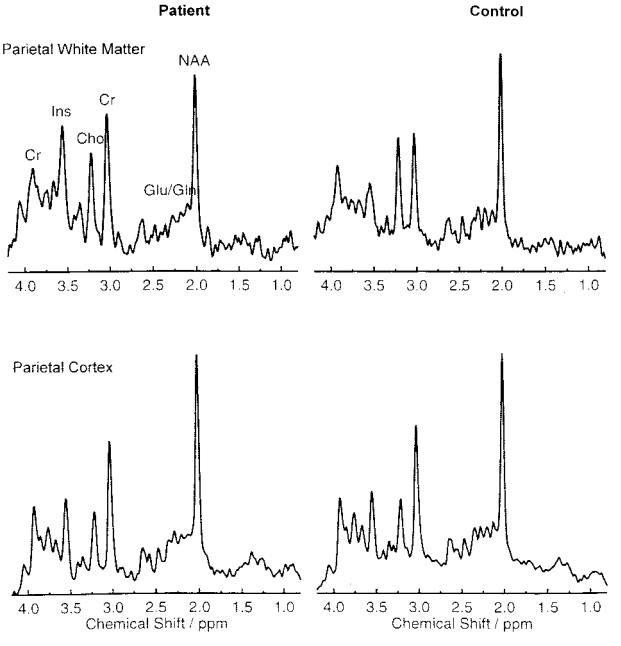

FIG 5. MR spectra in the parietal white matter (*top row*) and parietal cortex (*bottom row*) in patient 2 at age 7 years (*left*) compared with those in an age-matched control subject (*right*). All spectra are plotted on the same vertical scale to allow a qualitative comparison. Note the prominent increase in myo-inositol and Cr levels in the white matter, whereas the cortex spectrum is normal.

To our knowledge, the MR imaging pattern has not been described before. As Iwabuchi et al reported (25), autopsy findings in two siblings were similar to some degree. Degeneration of the cerebellar cortex, putamen, and caudate nucleus was found in combination with sparing of the globus pallidus, thalamus, and cerebral cortex. The cerebral white matter showed diffuse myelin pallor. However, the disease started later, in the fourth decade, and it was more rapidly progressive, leading to early death. The putamen was only mildly affected, whereas in our patients, the putamen was most severely involved. MR imaging findings were not described. Therefore, whether these patients had the same disease as that of our patients is not currently known.

Pathophysiology

The disease appears to be characterized by two processes: degeneration and a disturbance of normal development. Our patients' ages at MR imaging varied from 1 to 20 years, and follow-up data from a period as long as 10 years are available. The unchanging appearance of the myelin deficiency strongly suggests that the myelin never formed. Progressive atrophy of the cerebral white matter, putamen, caudate

nucleus, and cerebellum is documented. The disappearance of the basal ganglia without evidence of remaining scar tissue, as depicted on MR images, suggests atrophy by means of apoptosis rather than necrosis.

Both multiple single-voxel MR spectroscopy and MR spectroscopic imaging examinations were performed. The first provided higher quality spectral information, and the second provided information about the regional distribution of the three major metabolites seen with long-TE images (NAA, Cho, and Cr). The data suggest that the composition of the cerebral cortex is normal or nearly normal, with a relative decrease in NAA levels in the frontal region. These findings are compatible with the clinical impression of relatively preserved cortical function. In the cerebral white matter, the most striking findings are highly increased levels of myo-inositol and Cr. The increase in myo-inositol probably reflects gliosis (26, 27). The increased level of Cr suggests increased cellular density (28), probably with an increase in glial cells, which are the cells with the highest Cr levels (29). The normal NAA content of the cerebral white matter does not suggest substantial axonal damage (30, 31). The normal Cho level is not consistent with active demyelination (32); however, it is also unusual for hypomyelination. For instance, in Pelizaeus-Merzbacher disease, a decrease in the Cho level has been reported (33). An explanation for the normal Cho level in H-ABC could be that an increase in the Cho level due to glial proliferation compensates for the low Cho level associated with hypomyelination (29, 34). The basal ganglia spectra were obtained from the region where these nuclei are normally located. However, because of their small size, the VOI contained an admixture that included a considerable amount of white matter. In fact, the NAA levels in that region were similar to the white matter NAA levels.

No clinical, neurophysiologic, or morphologic evidence of hypomyelination of peripheral nerves is noted. The combination of a normal peripheral nerve conduction velocity and evoked potential findings with a decreased conduction velocity or absent recordable cortical responses is compatible with central hypomyelination (35). The results of the brain stem auditory evoked potential study are similar to those observed in Pelizaeus-Merzbacher disease (35).

The putative common factor responsible for the selective vulnerability of the central myelin, neostriatum, and cerebellum is unclear. Most hypomyelinating disorders are inherited. Although all seven patients are isolated cases and no consanguinity was shared among the parents, H-ABC is likely to be a genetically determined disorder. The variation in the clinical severity observed in our patients is not unusual for inherited disorders.

Conclusion

The highly distinctive pattern of MR imaging findings suggests that these patients' conditions represent one nosologic entity. The similarities in the clinical findings among the present patients is compatible with this hypothesis and allows for the possibility of severe and more benign variants. The acronym H-ABC is offered to indicate patients sharing these clinical and MR imaging features.

References

1. Van der Knaap MS, Breiter SN, Naidu S, et al. **Defining and categorizing leukoencephalopathies of unknown origin: MR imaging approach.** *Radiology* 1999;213:121–133
2. Kristjánsdóttir R, Uvebrant P, Hagberg B, et al. **Disorders of the cerebral white matter in children: The spectrum of lesions.** *Neuropediatrics* 1996;27:295–298
3. Fabrizi GM, Simonati A, Taioli F, et al. **PMP22 related congenital hypomyelinating neuropathy.** *J Neurol Neurosurg Psychiatry* 2001; 70:123–126
4. Volpe JJ. **Neuromuscular disorders.** In: *Neurology of the Newborn*. 4th ed. Philadelphia: W. B. Saunders; 2001:642–670
5. Van der Knaap MS, Valk J. **The reflection of histology in MR imaging of Pelizaeus-Merzbacher disease.** *AJNR Am J Neuroradiol* 1989;10:99–103
6. Schneck L, Adachi M, Volk BW. **Congenital failure of myelinization: Pelizaeus-Merzbacher disease.** *Neurology* 1971;21:817–824
7. Sonninen P, Autti T, Varho T, et al. **Brain involvement in Salla disease.** *AJNR Am J Neuroradiol* 1999;2:433–443
8. Nishio H, Kodama S, Matsuo T, et al. **Cockayne syndrome: magnetic resonance images of the brain in a severe form with early onset.** *J Inherit Metab Dis* 1988;11:88–102
9. Østergaard JR, Christensen T. **The central nervous system in Tay syndrome.** *Neuropediatrics* 1996;27:326–330
10. Van der Knaap MS, Valk J, de Neeling N, Nauta JJP. **Pattern recognition in magnetic resonance imaging of white matter disorders in children and young adults.** *Neuroradiology* 1991;33:478–493
11. Van der Knaap MS, Barth PG, Stroink H, et al. **Leukoencephalopathy with swelling and a discrepancy mild clinical course in eight children.** *Ann Neurol* 1995;37:324–334
12. Van der Knaap MS, Barth PG, Gabreëls FJM, et al. **A new leukoencephalopathy with vanishing white matter.** *Neurology* 1997;48: 845–855
13. Van der Knaap MS, Kamphorst W, Barth PG, et al. **Phenotypic variation in leukoencephalopathy with vanishing white matter.** *Neurology* 1998;51:540–547
14. Leegwater PAJ, Yuan BQ, Van der Steen J, et al. **Mutations of *MLC1* (KIAA0027), encoding a putative membrane protein, cause megalencephalic leukoencephalopathy with subcortical cysts.** *Am J Hum Genet* 2001;68:831–838
15. Leegwater PAJ, Vermeulen G, Könst AAM, et al. **Subunits of the translation initiation factor eIF2B are mutated in leukoencephalopathy with vanishing white matter.** *Nature Genet* 2001; 29:383–388
16. Van der Knaap MS, Leegwater PAJ, Könst AAM, et al. **Mutations in each of the five subunits of translation initiation factor eIF2B can cause leukoencephalopathy with vanishing white matter.** *Ann Neurol* 2002;51:264–270
17. Provencher SW. **Estimation of metabolite concentrations from localized in vivo proton MR spectra.** *Magn Reson Med* 1993;30:672–679
18. Pouwels PJW, Frahm J. **Regional metabolite concentrations in human brain as determined by quantitative localized proton MRS.** *Magn Reson Med* 1998;39:53–60
19. Pouwels PJW, Brockmann K, Kruse B, et al. **Regional age dependence of human brain metabolites from infancy to adulthood as detected by quantitative localized proton MRS.** *Pediatr Res* 1999; 46:925–928
20. Duyn JH, Gillen J, Sobering G, et al. **Multisection proton MR spectroscopic imaging of the brain.** *Radiology* 1993;188:277–282
21. Tedeschi G, Bertolino A, Righini A, et al. **Brain regional distribution pattern of metabolite signal intensities in young adults by proton magnetic resonance spectroscopic imaging.** *Neurology* 1995; 45:1384–1391
22. Van der Knaap MS, Valk J. **Magnetic resonance of myelin, myelination, and myelin disorders.** Heidelberg: Springer-Verlag; 1995
23. Barkovich AJ, Kjos BO, Jackson DE, Norman D. **Normal maturation of the neonatal and infant brain: MR imaging at 1.5 T.** *Radiology* 1988;166:173–180
24. Barkovich AJ. **Concepts of myelin and myelination in neuroradiology.** *AJNR Am J Neuroradiol* 2000;21:1099–1109

25. Iwabuchi K, Nakazawa Y, Akai J, et al. **Autosomal recessive hereditary cortical cerebellar atrophy with striatal degeneration - two siblings showing choreoathetoid movement, ataxia, dementia, and amenorrhea.** *No To Shinkei* 1994;46:563–571
26. Flogel U, Willker W, Leibfritz D. **Regulation of intracellular pH in neuronal and glial tumor cells, studied by multinuclear NMR spectroscopy.** *NMR Biomed* 1994;7:157–166
27. Brand A, Richter-Landsberg C, Leibfritz D. **Multinuclear NMR studies on the energy metabolism of glial and neuronal cells.** *Dev Neurosci* 1993;15:289–298
28. Wyss M, Kaddurah-Daouk R. **Creatine and creatine metabolism.** *Physiol Rev* 2000;80:1107–1213
29. Urenjak J, Williams SR, Gadian DG, Noble M. **Proton nuclear magnetic resonance spectroscopy unambiguously identifies different neural cell types.** *J Neurosci* 1993;13:981–989
30. Simmons ML, Frondoza CG, Coyle JT. **Immunocytochemical localization of N-acetylaspartate with monoclonal antibodies.** *Neuroscience* 1991;45:37–45
31. Van der Knaap MS, van der Grond J, Luyten PR, et al. **1H and 31P magnetic resonance spectroscopy of the brain in degenerative cerebral disorders.** *Ann Neurol* 1992;31:202–211
32. Davie CA, Hawkins CP, Barker GJ, et al. **Serial proton magnetic resonance spectroscopy in acute multiple sclerosis lesions.** *Brain* 1994;117:49–58
33. Spalice A, Popolizio T, Parisi P, et al. **Proton MR spectroscopy in connatal Pelizaeus-Merzbacher disease.** *Pediatr Radiol* 2000;30:171–175
34. Simone IL, Federico F, Tortorella C, et al. **Metabolic changes in neuronal migration disorders: evaluation by combined MRI and proton MR spectroscopy.** *Epilepsia* 1999;40:872–879
35. Nezu A. **Neurophysiology in Pelizaeus-Merzbacher disease.** *Brain Dev* 1995;17:175–181